

Climate-induced reversal of tree growth patterns at a tropical treeline

Paulo Quadri^{1,2*}, Lucas C. R. Silva³, Erika S. Zavaleta²

Globally, cold-limited trees and forests are expected to experience growth acceleration as a direct response to warming temperatures. However, thresholds of temperature limitation may vary substantially with local environmental conditions, leading to heterogeneous responses in tree ecophysiology. We used dendroecological and isotopic methods to quantify shifting tree growth and resource use over the past 143 years across topographic aspects in a high-elevation forest of central Mexico. Trees on south-facing slopes (SFS) grew faster than those on north-facing slopes (NFS) until the mid-20th century, when this pattern reversed notably with marked growth rate declines on SFS and increases on NFS. Stable isotopes of carbon, oxygen, and carbon-to-nitrogen ratios suggest that this reversal is linked to interactions between CO₂ stimulation of photosynthesis and water or nitrogen limitation. Our findings highlight the importance of incorporating landscape processes and habitat heterogeneity in predictions of tree growth responses to global environmental change.

INTRODUCTION

Subalpine tree species are particularly vulnerable to climate change because species in mountainous regions typically experience reduced climatic connectivity (1) and because they are at higher risk of experiencing mountaintop extinctions (2). Cold-limited subalpine forests are expected to expand upslope and/or experience growth acceleration in response to warming temperatures (3, 4). Increasingly, however, research has shown that upslope expansions and growth acceleration might not be a uniform response and that in many cases, subalpine tree species may instead rely more on the development of holdouts or *in situ* microrefugia for their persistence (5, 6). This variability challenges our ability to predict the future of subalpine forests under a warmer climate. It requires us to better link climate-driven shifts in the conditions and resources that limit species limiting conditions to changing ecophysiological and population-level responses.

Much attention has been given to the role of low temperatures in limiting subalpine species' distribution and growth and how, therefore, the combination of rising CO₂ concentrations and a warming climate should accelerate tree growth (7–10). However, findings in the literature include a mix of both growth acceleration and growth declines in subalpine forests (11–15). Similarly, although early work suggested that rising atmospheric CO₂ concentrations should stimulate tree growth and resource use efficiency (16), evidence of such stimulation has been mixed in natural ecosystems (11, 17–19).

One hypothesis for the lack of coherent responses in growth and resource use efficiency in high-altitude ecosystems is that regional CO₂ and warming effects are secondary to local hydrologic, biogeochemical, and ecological factors (17, 20–23). In montane landscapes, the latter factors can vary significantly with topography at small spatial scales, potentially generating spatially heterogeneous responses to warming and rising CO₂ (e.g., growth declines, growth acceleration, or no change). The importance of topographic aspect for tree growth and population dynamics has long been considered in mid- and high-latitude ecological research (24), while at lower

latitudes, the effect of aspect is typically viewed as less important and thus has received less attention (25, 26). At high latitudes, tree line habitats appear to have become more hospitable to tree recruitment and growth during the past century (27, 28). In contrast, at low latitudes, recent research suggests that tree line habitats will become less favorable for tree growth (29).

To advance basic understanding and ability to predict tree line responses, we used a combination of dendroecological and isotopic analyses to quantitatively reconstruct how contrasting local factors have affected tree growth and physiological performance across a tropical subalpine landscape over the past 143 years. We targeted dominant Hartwegii pines (*Pinus hartwegii*) in central Mexico at ~19°N latitude, sampling trees of different ages systematically on north- and south-facing landscape positions (Fig. 1). We then determined how variation in environmental conditions, including soil properties and associated differences in water and nutrient use across the landscape, interact to influence tree growth response to climate and rising atmospheric CO₂. We expected warming to positively affect tree growth, especially on north-facing slopes (NFS), which are colder and wetter habitats that receive less solar radiation. Correspondingly, we expected warmer and drier south-facing slope (SFS) habitats to experience more favorable conditions (relative to NFS trees), especially in recent decades because of rising temperatures and CO₂ levels (11, 30).

We examined the chemical composition of tree rings between aspects over time to assess the physiological mechanisms underlying potential changes in growth and link them to spatially and temporally varying resource availability. We used carbon isotope ratios (¹³C/¹²C) to reconstruct changes in intrinsic water use efficiency (iWUE) (31, 32) in tandem with oxygen isotope ratios (¹⁸O/¹⁶O), which indicate changes in water source (33). In addition, we used carbon-to-nitrogen (C:N) ratios in tree rings to examine nutrient limitation of photosynthesis (34), which commonly influences responses to rising CO₂ levels and climate variability in temperate ecosystems (35, 36). We relied on previous models of isotope enrichment in tree rings, which are commonly used to infer shifts in water supply (e.g., groundwater versus rain or snowmelt water) and subsequent acclimation of stomatal conductance (32). By combining these lines of evidence, we sought to understand the mechanisms

Copyright © 2021
The Authors, some
rights reserved;
exclusive licensee
American Association
for the Advancement
of Science. No claim to
original U.S. Government
Works. Distributed
under a Creative
Commons Attribution
NonCommercial
License 4.0 (CC BY-NC).

¹Sky Island Alliance, Tucson, AZ 85719, USA. ²University of California, Santa Cruz, Santa Cruz, CA 95064, USA. ³University of Oregon, Eugene, OR 97403, USA.
*Corresponding author. Email: pquadri@ucsc.edu, paulo@skyislandalliance.org

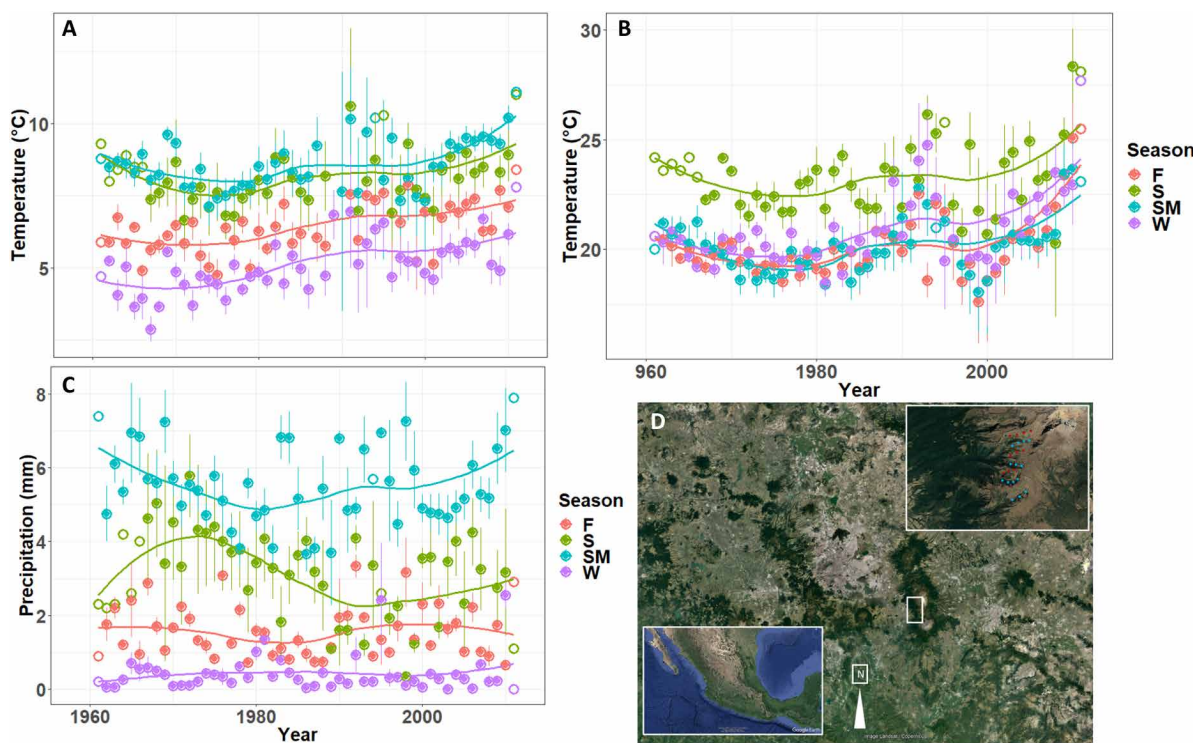


Fig. 1. Temperature and precipitation trends since 1960 and study region. Data collected from the nearest two weather stations (San Pedro Nexapa and Amecameca) located at ~2600 and ~2500 m above sea level, respectively: change in minimum (A) and maximum (B) temperatures and precipitation (C) by season (F, fall; S, spring; SM, summer; W, winter). Error bars represent SEs. (D) Location of study sites referenced within Mexico and the Mexico City Valley region. Images: Google Earth.

shaping tree growth responses to climate and CO₂ across subalpine landscapes.

RESULTS

Reversal of growth trends between aspects

We detected a relative reversal of growth trends between trees growing on different slope aspects (Fig. 2). Basal area increments (BAIs) on SFS were higher than those on NFS during the late 19th century and the first half of the 20th century (0.58 and 0.41 cm² year⁻¹, respectively) (fig. S1 and table S1). Starting in the 1930s, however, SFS pines began to show strong reductions in growth rates compared to NFS pines (−0.22 and −0.13 cm² year⁻¹, respectively) (fig. S1 and table S1). Growth limitations for SFS trees appeared to have increased in recent decades. After approximately 1980, growth rates stagnated in SFS trees (0.23 cm² year⁻¹), while they accelerated in NFS trees (0.019 cm² year⁻¹) (fig. S1 and table S1). This reversal in growth patterns between slope aspects is driven by differences in BAI between trees of similar age and does not reflect age-related changes in growth rate (fig. S3). Sampled trees varied in age ($N = 90$; range: 45 to 143 years) (fig. S2), with young NFS trees more likely to have experienced growth acceleration in recent decades than mature NFS trees (fig. S3A and table S2A). Accordingly, we found that on average, SFS trees reached larger diameters at an earlier age 60+ years ago compared to more recent years. Young trees on NFS showed the opposite pattern; they reached larger diameters at younger ages in recent years compared to in the past (fig. S3, B and C, and table S2B).

To facilitate comparison of growth rates and isotopic analyses between trees from different slope aspects, we grouped individuals

into three age classes: “mature,” “mid,” and “young.” We established these categories because three main recruitment events in the past century and a half could be discerned from the age distribution of all individuals (fig. S2). The duration of growth acceleration in currently young SFS was less than half that sustained by currently mature individuals (22 and 42 years, respectively). In contrast, currently young trees on NFS sustained BAI for 75 years, leading to the longest period of growth acceleration recorded in any of the three cohorts (1940–1982, 0.46 cm² year⁻¹; 1983–2015, 0.84 cm² year⁻¹) (table S3). In other words, today’s young SFS trees grew more slowly during their early years (in the 1950s and 1960s) than mature SFS trees did during their early years (in the late 1800s and early 1900s). Overall cross-correlations of our tree ring series had lower than usual values, with the highest values occurring within plots (table S4, A and B). This was expected since we designed our sampling to capture variation across topographic gradients, including different aspects and elevation, to be able to detect divergent responses to climate and CO₂ across landscape positions.

Carbon isotopes

On the basis of contrasting growth patterns between today’s mature and today’s young trees (table S3), we measured tree ring $\delta^{13}\text{C}$ values in trees belonging to these two age classes. $\delta^{13}\text{C}$ values of tree rings declined overtime in both mature and young individuals, reflecting atmospheric CO₂ enrichment (and accompanying depletion of $\delta^{13}\text{C}_{\text{air}}$) during the past century, although $\delta^{13}\text{C}$ values were always higher on SFS than on NFS (fig. S4 and table S5A). Atmosphere-to-plant discrimination of $^{13}\text{CO}_2$ ($\Delta^{13}\text{C}$) declined overtime in all trees, but discrimination was, on average, lower on SFS (Fig. 3 and table S5B). As expected, iWUE, calculated from $\Delta^{13}\text{C}$ values,

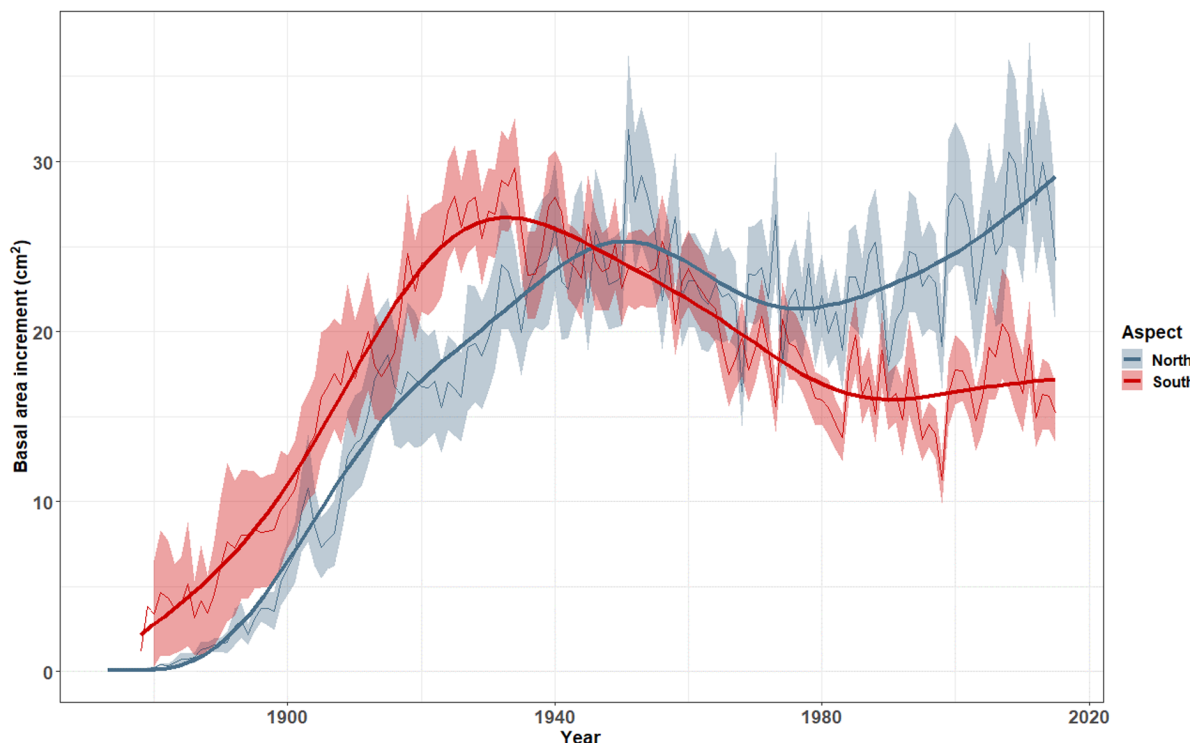


Fig. 2. Reversal of growth patterns between trees growing on contrasting topographic aspects. Growth trends are measured as BAI. Thin lines are mean values, and shaded areas represent SEs. Thick lines are fitted curves from a general additive model using “year” and “aspect” as smoothing terms.

increased significantly overtime in all trees regardless of slope aspect. However, in mature individuals, iWUE was, on average, higher on SFS, while in young individuals, this pattern across aspects was initially absent and became more evident with time (Fig. 3 and tables S5A and S6A). When compared to a simulated baseline of WUE based on constant relationship between intracellular CO_2 concentrations and atmospheric CO_2 concentrations (C_i/C_a ratios depicted as gray triangles in Fig. 3), NFS trees, especially young individuals, showed weaker stomatal regulation of gas exchange compared to SFS trees (Fig. 3).

Oxygen isotopes

Tree ring (whole wood) oxygen isotope ratios ($\delta^{18}\text{O}$) increased over time only in mature trees on SFS, pointing at potential gradual, evaporative enrichment of ^{18}O (Fig. 4 and table S6B). This finding suggests a potential increase in water conservation (i.e., increasingly low stomatal conductance and transpiration) in mature but not young SFS trees. However, the lack of statistical trends indicates that no significant changes in source water occurred despite large variability and different $\delta^{18}\text{O}$ values between trees of different ages and on different slope aspects.

C:N ratios

Tree ring (whole wood) C:N ratios increased sharply in mature NFS trees between 1876 and 1933 and then steadily declined from 1934 to 2015 (Fig. 5 and table S6C). On SFS, however, mature trees showed a significant decline in C:N ratios only after 1954 (Fig. 5 and table S6, C and D). Young SFS trees showed a sharp decline in C:N ratios, whereas NFS young trees showed increasing C:N ratios (Fig. 5 and table S6E).

iWUE and growth

Unlike tree ring-based climatological reconstructions, our study focused on quantifying variation in sensitivity to climate and CO_2 among sites across landscape positions with different environmental conditions. Thus, we analyzed the response of iWUE as a mixed-effects linear function of the interaction between either mean maximum annual temperature or mean annual precipitation and aspect, with tree size and tree age as fixed effects and year and tree ID as random effects. In any given year, iWUE increased with higher mean maximum temperatures, but this effect was stronger in SFS trees than on NFS (0.623 ± 0.162 ; $P < 0.001$) (Table 1). Precipitation had stronger effects on iWUE of SFS trees than of NFS trees, with wetter years reducing iWUE (-2.77 ± 1.03 ; $P = 0.0079$) (Table 1). Warmer years led to reduced BAI in SFS relative to NFS (-1.042 ± 0.147 ; $P < 0.001$). These trends and magnitudes in iWUE and BAI were also maintained when we included 1-year lags of temperature and precipitation (table S9). Last, in any given year, greater iWUE was associated, on average, to reduced growth on SFS relative to NFS trees (-1.91 ± 0.174 ; $P < 0.001$) (table S7 and fig. S5).

DISCUSSION

We found divergent responses to climate change between aspects in a tree line forest ecotone. Beginning in the 1880s, our dendrochronological records suggest that warming temperatures led to an initial increase in tree growth across all sites during the first half of the 20th century (especially on SFS). However, a reversal in tree growth occurred after the 1950s when NFS became more favorable than SFS to tree growth. This result contrasts with the notion that tree growth in tree line ecosystems responds positively to warming

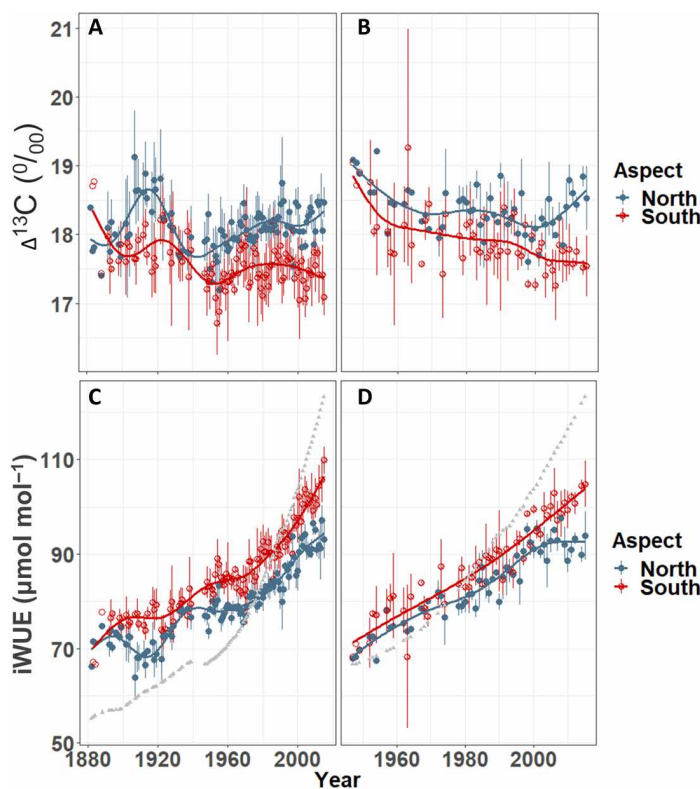


Fig. 3. Understanding shifting limiting conditions through the lens of stomata regulation. (A and B) $\Delta^{13}\text{C}$ discrimination ($\Delta^{13}\text{C}$) of mature and young individuals by slope aspect showing less discrimination on south aspect trees relative to north aspects (see table S6A). Lines are generalized additive model fit. (C and D) Calculated iWUE from $\Delta^{13}\text{C}$ values in mature and young trees, respectively, growing on north and on south aspects. Values are plotted alongside a simulated baseline of constant C_i/C_a (gray triangles). Lower values relative to that line suggest weaker stomatal regulation of gas exchange.

temperatures (37, 38). It shows that responses to elevated CO_2 are not only species specific (39) but also specific to local environmental conditions. We found that tree growth rates declined on SFS within 5 to 10 years of a recent acceleration in NFS growth rates, marking a recent shift in temperature sensitivity. This reversal in growth rates between different topographic positions was likely caused by a consistent increase in air temperature (Fig. 1, A and B) and an overall decline in summer precipitation (Fig. 1C) in recent decades. We posit that local variation in soil moisture regime modulated tree growth responses to rising temperatures. Soil moisture declines outweighed any potential CO_2 stimulation effect on SFS tree growth but did not do this on NFS, where current conditions still favor accelerating tree growth.

Contrary to expectations, we did not find clear growth signals of El Niño–Southern Oscillation events, which have been recorded in other montane forests in the region (40). We lack historical climate data before the 1960s, when the local instrumental record begins, but our growth data indicate a persistent trend from favorable to increasingly adverse conditions on SFS and increasingly favorable conditions on NFS. These correlate well with variation in ecophysiological performance inferred from tree ring isotope ratios (discussed below). Our finding is consistent with modeled hierarchical constraints on tree and forest carbon-water relations (41), which postulated that soil properties that regulate landscape variation in

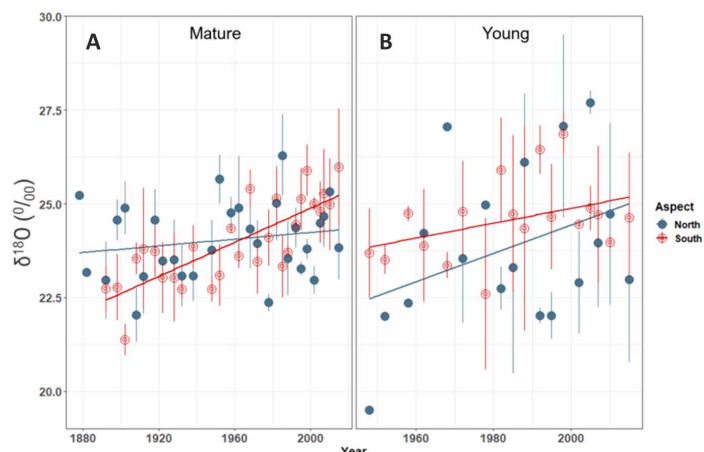


Fig. 4. Increasing evapotranspiration on mature south aspect trees revealed by tree ring $\delta^{18}\text{O}$ values. (A) The only significant trend, reflecting a potential gradual evaporative enrichment, occurred on south aspect mature trees only ($P = 0.0103$). (B) High variability in young individuals suggesting that no significant changes in source water occurred during the study period. Error bars represent SEs.

water holding capacity and moisture dynamics (e.g., organic matter, texture, and depth) became increasingly important in influencing tree growth as warming progressed over the past century. Divergent growth responses between SFS and NFS were more pronounced for the younger cohorts of trees, which suggests that mature trees are more resilient to the observed changes in climate. We speculate that deeper and broader root systems may be one of the mechanisms driving these age-dependent patterns. Alternatively, trees could be allocating carbon to nonstructural carbohydrate reserves, as found for other tree species where temperature-assisted carbohydrate allocation links environmental cues and tree phenology, providing a thermal metabolic fine-tuning in simulated seasons (42). Future empirical and modeling studies stand to gain valuable information from testing these hypotheses in climate-sensitive ecotonal systems.

Carbon isotopes

The iWUE of trees growing on SFS increased consistently over time, but the iWUE trend for NFS declined in recent decades, especially for young trees (Table 1A and Fig. 3, C and D). This suggests a trade-off between productivity and iWUE, in which tree growth acceleration was most pronounced when stomatal control of transpiration became weak, leading to divergent trends in carbon isotope discrimination ($\Delta^{13}\text{C}$; Fig. 3). While increasing iWUE is expected from rising CO_2 concentrations (C_a), the comparison of aspects allowed us to infer the modulating effect of other environmental factors on intercellular CO_2 concentrations (C_i), such as water limitation leading to a decline in $\Delta^{13}\text{C}$ or increasing water availability and transpiration leading to an increase in $\Delta^{13}\text{C}$. Given the relationships between temperature, precipitation, and growth described above, it is likely that the aspect-dependent differences in iWUE that were not accounted for by increasing C_a are a consequence of drought stress. We show this by comparing measured values of iWUE to modeled values assuming constant C_i/C_a relationships, indicating stronger stomatal regulation of gas exchange (i.e., closer to the modeled constant C_i/C_a curve) in SFS trees relative to NFS ones. The iWUE of all trees across the landscape fell above the modeled C_i/C_a values until the recent reversal of tree growth in the 1960s, at which point, differences in iWUE became more pronounced between aspects.

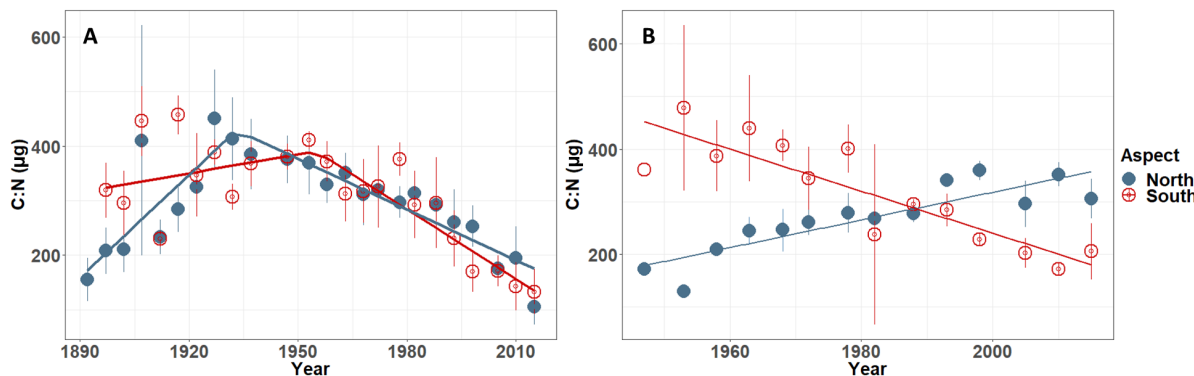


Fig. 5. On north aspect trees, periods of growth correlate with decreasing tree ring N concentrations. Higher nitrogen concentrations in wood lead to lower C:N ratios. Data show mean values of measured C:N ratios from multiple trees (four on each aspect). Error bars represent SEs. Regression lines in (A) are from separate piecewise regression models on each aspect. On (B), regression lines are from simple linear regression for each aspect.

The onset of growth rate declines in mature trees was similar across aspects. SFS trees declined in growth rate in 1927, after 45 years of growth acceleration (table S3), when trees reached iWUE of $\sim 78 \mu\text{mol mol}^{-1}$. Tree growth decline began in 1932 on NFS, after 56 years of growth acceleration, and again initiated when trees reached iWUE of $\sim 78 \mu\text{mol mol}^{-1}$. In contrast, currently young trees showed remarkable and entirely different aspect-related patterns. For young SFS trees, growth declines began in 1961 (table S3), not only after 21 years of initial growth acceleration but also when they reached iWUE of $\sim 78 (\mu\text{mol mol}^{-1})$. However, young NFS trees continued to experience growth acceleration after 77 years of establishment (table S3), recording iWUE levels of $\sim 91 (\mu\text{mol mol}^{-1})$ during the past few years. In other words, SFS trees experienced growth declines regardless of their age when they reached iWUE of approximately $78 (\mu\text{mol mol}^{-1})$. By contrast, young NFS trees have been able to maintain fast growth rates at $\sim 44\%$ higher iWUE levels than those found for the mature individuals during their initial period of growth acceleration (1876 to 1932).

Recent changes in iWUE and growth declines suggest that SFS trees could be entering an “isohydric trap” in which soil water or nutrient limitation begins to occur because of high water potentials after prolonged conditions of high evaporative demand (43). As with other tree line-forming species, *P. hartwegii* has been found to lack cross-population genetic differentiation for cavitation resistance (44), potentially leaving stomatal regulation of transpiration as their main drought-coping strategy. Conversely, the weak stomatal regulation shown by NFS trees suggests that a synergy among warmer temperatures, CO_2 fertilization, and local soil moisture and nutrients may have favored recent tree growth acceleration. This explanation for cross-aspect differences is supported by the observed positive effect of spring precipitation on growth in SFS trees and the observed positive effect of warmer minimum temperatures on NFS tree growth.

We focused our isotopic analyses on mature and young trees only because these cohorts showed the greatest contrasts in growth trends. However, it is possible that additional isotopic analyses on the mid-age cohort (trees established around 1920) could provide further insights into the mechanisms behind the growth reversal trend across slope aspects.

Oxygen isotopes

We expected $\delta^{18}\text{O}$ to increase over time with iWUE and temperature trends, especially on SFS. This would support a hypothesis of

increasing temperatures limiting stomatal conductance and increasing evaporative enrichment of oxygen isotopes in leaf water and photosynthetic compounds (45). We found $\delta^{18}\text{O}$ enrichment in tree rings of mature cohorts on SFS but not on NFS. This result, combined with the lack of a clear pattern of enrichment in young trees, indicates that the differences in $\delta^{18}\text{O}$ values between cohorts are physiological and cannot be explained by regional variations in isotopic signatures of precipitation over time. Although higher winter precipitation was correlated with $\delta^{18}\text{O}$ depletion in NFS tree rings and with $\delta^{18}\text{O}$ enrichment in SFS (fig. S7), we found no significant effect of winter precipitation or maximum summer and spring temperatures on $\delta^{18}\text{O}$. The lack of $\delta^{18}\text{O}$ signal contrasts with the marked differences in $\Delta^{13}\text{C}$ and iWUE in response to climatic and topographic variables. It is unexpected because the variation in $\Delta^{13}\text{C}$ and iWUE that we observed was consistent with differences in solar radiation and temperature between south- and north-facing landscape positions. Accordingly, we expected that $\delta^{18}\text{O}$ values in SFS trees would reflect enhanced stomatal regulation and cumulative transpiration as part of an isohydric drought-coping strategy (43). One possible explanation for our result is that dominant trees with more exposed canopies, on previously more productive SFS trees, are the most susceptible to isotopic fractionation that is known to occur during evapotranspiration (46). Given variation in source water $\delta^{18}\text{O}$, it is difficult, if not impossible, to detect differences across this relatively small topographic gradient and to confidently isolate specific ecophysiological controls.

Resources limiting sensitivity to climate and CO_2

A key conclusion of this study is that rising temperatures and CO_2 concentrations do not necessarily translate into tree growth acceleration. Instead, critical interactions between changing environmental conditions at global and regional scales (i.e. temperature, precipitation, and CO_2) and local environmental heterogeneity (i.e., local topography) are likely to produce variable outcomes, even within populations of long-lived organisms such as trees. At higher latitudes, tree growth acceleration in subalpine trees has been attributed to synergies between C_a and increasing water and nitrogen availability from thawing permafrost soils (11). In our case, growth acceleration is accompanied by increasing wood C:N ratios, which indicate decreasing N concentrations over time for mature trees growing on both aspects. Therefore, changes in C:N ratios do not explain the observed reversal in growth trajectories across our sites.

Table 1. Differential effects of temperature and precipitation on tree ecophysiology based on slope aspect. Summary of mixed-effects models showing the habitat-specific magnitude and direction of the effects of climate variables on (A) iWUE and (B) BAI. Higher temperatures make all trees more water use efficient but more so on south aspects. Less cold years favor growth of trees on north-facing aspects. More precipitation makes all trees less water use efficient but especially south aspect trees. More precipitation also increases growth on south aspects relative to north aspects. ICC, intraclass correlation coefficient.

(A)									
Predictors	Temperature				Precipitation				P
	iWUE (mmol/mol)				iWUE (mmol/mol)				
(Intercept)	48.0497	7.0356	6.8295	<0.001	94.1427	6.0395	15.5877	<0.001	
Mean annual max. temp	1.5002	0.2864	5.2389	<0.001					
Aspect [south]	-7.8136	3.95	-1.9781	0.0501	12.1106	2.9478	4.1083	0.0002	
Tree size	0.0603	0.0737	0.8185	0.4441	0.0594	0.0737	0.8066	0.4504	
Tree age	0.0154	0.0279	0.5509	0.6012	0.0161	0.0279	0.5792	0.5832	
Mean annual max. temp * aspect [south]	0.6233	0.1628	3.8291	0.0001					
Mean annual precipitation					-5.9019	2.1804	-2.7068	0.009	
Mean annual precipitation * aspect [south]					-2.7747	1.0391	-2.6704	0.0079	
Random effects									
σ^2			18.43				18.74		
τ^00			21.77 CO2.mean				33.92 CO2.mean		
			5.78 TreelD				5.76 TreelD		
ICC			0.47 CO2.mean				0.58 CO2.mean		
			0.13 TreelD				0.10 TreelD		
Observations			460				460		
Marginal R^2 /conditional R^2			0.412/0.764				0.251/0.760		
(B)									
Predictors	Temperature				Precipitation				P
	BAI (cm ²)				BAI (cm ²)				
(Intercept)	-9.5589	4.2518	-2.2482	0.0257	14.3815	3.7625	3.8223	0.0002	
Mean annual max. temp	0.8741	0.1312	6.6635	<0.001					
Aspect [south]	19.129	3.4773	5.5011	<0.001	-11.751	2.5519	-4.6046	<0.001	
Tree size	0.8482	0.0498	17.031	<0.001	0.8482	0.0498	17.0354	<0.001	
Tree age	-0.2925	0.0319	-9.1701	<0.001	-0.2928	0.0319	-9.1793	<0.001	
Mean annual max. temp * aspect [south]	-1.0422	0.1478	-7.0535	<0.001					
Mean annual precipitation					-2.1489	0.8818	-2.437	0.0166	
Mean annual precipitation * aspect [south]					3.5814	0.9327	3.84	0.0001	
Random effects									
σ^2			156.84				158.06		
τ^00			37.63 TreelD				37.59 TreelD		
			2.01 CO ₂				2.79 CO ₂		
ICC			0.19 TreelD				0.19 TreelD		
			0.01 CO ₂				0.01 CO ₂		
Observations			4642				4642		
Marginal R^2 /conditional R^2			0.425/0.541				0.419/0.537		

In young trees, however, growth acceleration coincided with a significant increase in C:N ratios (Fig. 4). One possible explanation for this observation is a potential increase in nitrogen use efficiency (NUE). Increasing NUE has been shown to occur with increasing C_a (47) for some evergreen conifers, which store most of their N in their youngest needles (48). The observed trends in C:N in our study are consistent with a scenario of sufficient soil moisture and increasing NUE on NFS rather than of a potential decline in soil N availability. While previous studies suggest that NUE in conifers typically increases with iWUE, the combination of growth acceleration and increasing C:N ratios observed in young NFS trees point to a productivity-efficiency trade-off that deserves further exploration.

Our results imply that photosynthetic stimulation in response to increasing C_a occurs only under specific edaphic and climatic conditions, which can be predicted from geographic information such as landscape position. Specifically, we show that disparate results can occur across small spatial scales and across different generations within a population, adding complexity to current understanding of species responses to climate and atmospheric changes. Together, our findings highlight the risks of making regional or global predictions of high-altitude forest species responses to climate change without accounting for landscape variation. The detection of shifting growth patterns and their associated limiting factors highlight how climate change can affect thresholds of ecological stability across spatial and temporal scales. At the same time, these shifts point to a potential link between physiological responses and the future distribution of pine forests at low latitudes. Along with other recent studies from Mediterranean and temperate regions (11, 20, 27, 49), the low-latitude sites studied here indicate that as CO₂ and temperatures continue to rise, NFS may become climatic holdouts or microrefugia. Incorporating these and other relevant findings into niche theory and species distribution models should be a priority for conservation strategies for protected areas and management plans.

Our results also add to the discussion about a potential latitudinal gradient that mediates the influence of aspect on the responses of tree line species to climate change. In Canada's southwest Yukon region, Danby and Hik (28) observed rapid tree line advancement on SFS. In the Colorado Rocky Mountains, pulses of tree line advancement between aspects were more frequent on SFS but depended on variation in water deficit (27). Further south, we found growth declines and stagnation on SFS. As warming progresses, mid and high latitudes may begin to experience similar trends to those that we found in Mexico at lower latitudes. The persistence of glaciers and snowpack at the highest elevations or latitudes may buffer habitats from warming-induced stress during the growing season, at least temporarily (50). In other systems, these buffering effects have resulted in lagged responses of plant community composition and productivity to climate change (51). In montane forests of central Mexico, this buffering effect influenced tree response to the driest and wettest events since 1850, manifested as a 3- to 10-year lag in BAI growth responses accompanied in some cases by iWUE and $\delta^{18}\text{O}$ excursions (40). In recent decades, glaciers in the volcanoes of central Mexico have almost disappeared. This may have had an additional negative impact on trees that would otherwise be able to persist in water-limited habitats (52).

Summary and future directions

Understanding how local-scale environmental heterogeneity mediates species responses to climate change is fundamental to predicting

ecological and biogeochemical dynamics in montane ecosystems (53). Our data will advance the prioritization of landscapes for in situ microrefugia, which are increasingly important in preventing regional extinctions and securing ecosystem resilience (54–56). Subalpine tree species are especially vulnerable to climatic and atmospheric changes because they are at higher risk of suffering mountaintop extinctions (57). However, our study illustrates how local-scale environmental factors and population characteristics interact and mediate tree line species responses to global climate changes. This underscores the need for more integrated, multiscale research integrating field ecology and modeling to better predict and prioritize in situ microrefugia in high-altitude forest ecosystems. Our results are limited in their ability to predict large-scale responses across tree line ecosystems. However, they inform future research that could transform our understanding of how multiscale ecological and biogeochemical interactions modulate climate-induced changes in species distributions, improving prediction of changes in ecosystem structure and function.

MATERIALS AND METHODS

Description of study sites

Our study site was located approximately 70 km southeast of Mexico City, in Iztaccíhuatl–Popocatépetl (Izta–Popo) National Park (19°07'43", 98°39' 37") in the Trans-Mexican Volcanic Belt ecoregion of central Mexico, between the states of Puebla and Mexico (Fig. 1). The research area spans an altitudinal gradient between 3600 and 3950 m above sea level. At the lowest elevations of this gradient, *P. hartwegii* forest is met by a montane forest dominated by "sacred" firs (*Abies religiosa*). At their upper distributional limit, the pines thin gradually into a system of alpine grasslands dominated by *Festuca tolucensis* and *Muhlenbergia quadridentata*. Other important understory species are *Lupinus montanus* and *Senecio spp.* The local climate is considered subhumid temperate, characterized by cool, wet summers with rains beginning in early June and extending to October or November. Mean annual precipitation is 928 mm, and mean annual temperature on the lower slopes is 14° and 5°C above 4000 m above sea level (58). The warmest months in this region are April and May, which typically also record the greatest evaporation rates (fig. S6, C and D).

Sampling design

We used a systematic sampling design along the western canyons of the Iztaccíhuatl volcano. We used six transects, three on SFS and three on NFS. On average, transects spanned 1.2 km of distance and 200 m of altitudinal change. On each transect, we worked on three to four plots of radius 15 to 20 m and at ~250 intervals of Euclidean distance between them to collect two increment cores of 5 and 12 mm at ~1.3 m above ground level from each of the five or four *P. hartwegii* individuals with the least amount of apparent biological or physical damage and representing multiple size classes all with diameter at breast height >10 cm ($N = 90$ trees; SFS, 45; NFS, 45).

Sample processing and growth measurements

Tree cores were mounted, sanded, and polished, and ring width measurements were performed on high-resolution scanned images using ImageJ (software info). Cross-dating analyses were done using the dplR package in R (59). We converted raw ring width measurements into BAI. The use of BAI provides accurate metrics for

aboveground tree productivity. Because it detrends ontogenetic effects from ring widths, it reliably estimates growth throughout the tree life span (60). BAI was calculated as follows

$$BAI = \pi * (R_t^2 - R_{t-1}^2) \quad (1)$$

where R is the tree radius and t is the year of ring formation. The formula assumes basal uniformity of annual increments.

Isotopic and nutrient measurements

We selected eight individuals on the basis of our BAI analyses (four from each aspect habitat; two mature and two young individuals) representing the most contrasting growth patterns across the landscape. Individual rings of each tree were sliced off the tree cores and ground as whole wood. Processing samples as whole wood, instead of purified cellulose, allowed us to prioritize resources and focus on replication and depth of our stable isotopic analysis without necessarily sacrificing analytical accuracy (61). We used carbon isotopes to understand changes in iWUE and its potential relationship to changing growth patterns. For carbon isotopes, we generated yearly resolutions between 1978 and 2015 to capture the growth reversal pattern. Between 1878 and 1978, we selected rings on the basis of periods of divergence and convergence between both habitats. We used analyses of oxygen isotopes and nitrogen in tandem with carbon isotopes to assist in the identification of mechanisms behind changes in growth (11, 32). Isotopic analyses were performed at the Stable Isotope Facility of the University of California, Davis. Carbon isotope analyses are characterized as follows

$$\delta ({}^{\text{o}}/\text{oo}) = (R_{\text{sample}} - R_{\text{standard}} - 1) * 1000 \quad (2)$$

where R_{sample} and R_{standard} are the carbon isotopic ratios in the sample material and a reference standard, respectively (the Vienna Pee Dee Belemnite formation for $\delta^{13}\text{C}$ and the Vienna Standard Mean Ocean Water for $\delta^{18}\text{O}$). For meaningful interpretations of carbon isotopes, the following derivations are necessary to correct for changes in atmospheric $\delta^{13}\text{C}$ (32, 62)

$$\Delta^{13}\text{C} = (\delta^{13}\text{C}_{\text{air}} - \delta^{13}\text{C}_{\text{plant}}) / (1 + \delta^{13}\text{C}_{\text{air}} / 1000) \quad (3)$$

where $\Delta^{13}\text{C}$ is the discrimination against ^{13}C , $\delta^{13}\text{C}_{\text{air}}$ represents the isotopic ratio of the atmosphere (the source), and $\delta^{13}\text{C}_{\text{plant}}$ is the isotopic ratio of plant biomass (the product). Isotopic discrimination, in turn, is described as follows

$$C_i = C_a * (\Delta^{13}\text{C} - a) / (b - a) \quad (4)$$

where a is the discrimination against $^{13}\text{CO}_2$ occurring through stomata diffusion during the gaseous phase ($4.4\text{ }{}^{\text{o}}/\text{oo}$) and b is the net discrimination occurring during carboxylation ($27\text{ }{}^{\text{o}}/\text{oo}$).

Last, iWUE is given by

$$\text{iWUE} = A / g = C_a * [1 - (C_i / C_a)] * 0.625 \quad (5)$$

where A is net carboxylation, g is leaf stomatal conductance, and 0.625 is the constant relating conductance of CO_2 molecules and water vapor. $\Delta^{13}\text{C}$ in plants is directly related to changes in C_i / C_a at the leaf level, which, as described above, is controlled by the net assimilation rate (A) and stomatal conductance (g). Therefore, changes

in ^{13}C discrimination can be caused either by drought conditions (affecting mostly stomata conductance) or by changes in nutrition or temperature (mostly related to net assimilation rate) (32). In addition, we compared our iWUE data to a simulated baseline of WUE in which C_i / C_a are held constant, above which measured values indicate a relatively stronger stomatal control of gas exchange, attributed to decreasing water availability in the case of SFS trees (from Eq. 5) (63).

Climate data

Temperature and precipitation data by season between 1961 and 2015 were obtained from the closest weather stations to the field sites (San Pedro Nexapa station, ~9 km southwest and 2600 m above sea level, and Amecameca station, ~8 km west and 2500 m above sea level), and missing records were completed using the next closest stations. Global CO_2 concentrations and $\delta^{13}\text{C}_{\text{air}}$ values were obtained from existing publications (64) and complemented with data from the National Oceanic and Atmospheric Administration's CarbonTracker, version CT2017 (65). To confirm temperature differences between aspects, we calculated mean incident annual radiation using a 15-m resolution digital elevation model in ArcMap 10.3.1 (fig. S6A) and measured near-surface temperature (at 0.5-m height from the ground) between January 2016 and February 2017 using temperature microloggers (Thermochron sensors; three on SFS and four on NFS) (fig. S6B).

Statistical analyses

We performed the standardization of tree ring measurements using the C-method (66) and selected the cohorts on the basis of the distribution of age frequencies (fig. S2). We used generalized additive models to analyze trends in growth and ecophysiological variables derived from carbon isotopes. When needed, we also used least squares regressions and piecewise regression to evaluate and compare growth rates and changes in isotopic values through interactions among aspect habitats and cohorts over the different periods of interest. Adjusted coefficients of determination (r^2), estimates, and probabilities are reported where appropriate. We generated two pairwise correlation matrices, one per slope aspect, to explore the strength and direction of association between different environmental and ecophysiological variables during the past 55 years, for which weather station records exist (fig. S7). We then developed two sets of mixed-effects models to analyze the effect of these parameters on our main response variables: growth and iWUE (Table 1). The first set analyzes iWUE, and the second analyzes BAI, both using either mean annual maximum temperature or mean annual precipitation interacting with aspect as fixed effects and CO_2 and tree ID as random effects (Tables 1). We favored the use of mixed-effect models to analyze relationships between ecophysiological and climate variables because our tree ring data have multiple sources of random variability, including variability within aspect, within plots, and within each tree across time. Additional sets of mixed-effects models were used to further explore intra-annual climate variables by slope aspect (table S8). Spring temperatures were used for SFS because this is the hottest season in central Mexico and thus has the most ecological significance for SFS trees (fig. S6). Winter temperature and fall precipitation were used as main predictors for NFS trees, as these were the most relevant variables to our hypotheses. For all analyses, we used R (R Core Team, 2012) and lme4 (67) to perform linear mixed-effects analyses and the mgcv package (68) to perform generalized additive models.

SUPPLEMENTARY MATERIALS

Supplementary material for this article is available at <http://advances.sciencemag.org/cgi/content/full/7/22/eabb7572/DC1>

REFERENCES AND NOTES

1. S. Z. Dobrowski, S. A. Parks, Climate change velocity underestimates climate change exposure in mountainous regions. *Nat. Commun.* **7**, 12349 (2016).
2. E. Rehm, K. J. Feeley, Many species risk mountain top extinction long before they reach the top reach the top. *Front. Biogeogr.* **8**, e27788 (2016).
3. J. Lenoir, J. C. Gégout, P. A. Marquet, P. De Ruffray, H. Brisse, A significant upward shift in plant species optimum elevation during the 20th century. *Science* **320**, 1768–1771 (2008).
4. D. D. Breshears, T. E. Huxman, H. D. Adams, C. B. Zou, J. E. Davison, Vegetation synchronously leans upslope as climate warms. *Proc. Natl. Acad. Sci. U.S.A.* **105**, 11591–11592 (2008).
5. L. Hannah, L. Flint, A. D. Syphard, M. A. Moritz, L. B. Buckley, I. M. McCullough, Fine-grain modeling of species' response to climate change: Holdouts, stepping-stones, and microrefugia. *Trends Ecol. Evol.* **29**, 390–397 (2014).
6. M. B. Ashcroft, Identifying refugia from climate change. *J. Biogeogr.* **37**, 1407–1413 (2010).
7. C. Körner, J. Paulsen, A world-wide study of high altitude treeline temperatures. *J. Biogeogr.* **31**, 713–732 (2004).
8. B. Ohse, F. Jansen, M. Wilming, Do limiting factors at Alaskan treelines shift with climatic regimes? *Environ. Res. Lett.* **7**, 015505 (2012).
9. F. Holtmeier, G. Broll, Sensitivity and response of Northern Hemisphere altitudinal and polar treelines to environmental change at landscape and local scales. *Glob. Ecol. Biogeogr.* **14**, 395–410 (2005).
10. J. Paulsen, U. M. Weber, C. Körner, Tree growth near treeline: Abrupt or gradual reduction with altitude? *Arct. Antarct. Alp. Res.* **32**, 14–20 (2000).
11. L. C. R. Silva, G. Sun, X. Zhu-Barker, Q. Liang, N. Wu, W. R. Horwath, Tree growth acceleration and expansion of alpine forests: The synergistic effect of atmospheric and edaphic change. *Sci. Adv.* **2**, e1501302 (2016).
12. A. Gómez-Guerrero, L. C. R. Silva, M. Barrera-Reyes, B. Kishchuk, A. Velázquez-Martínez, T. Martínez-Trinidad, F. O. Plascencia-Escalante, W. R. Horwath, Growth decline and divergent tree ring isotopic composition ($\delta^{13}\text{C}$ and $\delta^{18}\text{O}$) contradict predictions of CO_2 stimulation in high altitudinal forests. *Glob. Chang. Biol.* **19**, 1748–1758 (2013).
13. E. Liang, C. Leuschner, C. Dulamsuren, B. Wagner, M. Hauck, Global warming-related tree growth decline and mortality on the north-eastern Tibetan plateau. *Clim. Chang.* **134**, 163–176 (2016).
14. C. Dulamsuren, M. Hauck, G. Kopp, M. Ruff, C. Leuschner, European beech responds to climate change with growth decline at lower, and growth increase at higher elevations in the center of its distribution range (SW Germany). *Trees* **31**, 673–686 (2017).
15. A. Fajardo, E. J. B. McIntire, Reversal of multicentury tree growth improvements and loss of synchrony at mountain tree lines point to changes in key drivers. *J. Ecol.* **100**, 782–794 (2012).
16. B. G. Drake, M. A. González-Meler, S. P. Long, More efficient plants: A consequence of rising atmospheric CO_2 ? *Annu. Rev. Plant Physiol. Plant Mol. Biol.* **48**, 609–639 (1997).
17. J. Peñuelas, J. G. Canadell, R. Ogaya, Increased water-use efficiency during the 20th century did not translate into enhanced tree growth. *Glob. Ecol. Biogeogr.* **20**, 597–608 (2011).
18. P. Van Der Sleen, P. Groenendijk, M. Vlam, N. P. R. Anten, A. Boom, F. Bongers, T. L. Pons, G. Terburg, P. A. Zuidema, No growth stimulation of tropical trees by 150 years of CO_2 fertilization but water-use efficiency increased. *Nat. Geosci.* **8**, 24–28 (2015).
19. C. Körner, Carbon limitation in trees. *J. Ecol.* **91**, 4–17 (2003).
20. E. G. de Andrés, J. J. Camarero, U. Büntgen, Complex climate constraints of upper tree line formation in the Pyrenees. *Trees* **29**, 941–952 (2015).
21. T. M. Maxwell, L. C. R. Silva, W. R. Horwath, Integrating effects of species composition and soil properties to predict shifts in montane forest carbon–water relations. *Proc. Natl. Acad. Sci. U.S.A.* **115**, E4219–E4226 (2018).
22. H. Loranger, G. Zottz, M. Y. Bader, Early establishment of trees at the alpine tree line: Idiosyncratic species responses to temperature–moisture interactions. *AoB PLANTS* **8**, plw053 (2016).
23. R. A. Andrus, B. J. Harvey, K. C. Rodman, S. J. Hart, T. T. Veblen, Moisture availability limits subalpine tree establishment. *Ecology* **99**, 567–575 (2018).
24. J. Bennie, B. Huntley, A. Wilshire, M. O. Hill, R. Baxter, Slope, aspect and climate: Spatially explicit and implicit models of topographic microclimate in chalk grassland. *Ecol. Model.* **216**, 47–59 (2008).
25. J. A. Gallardo-Cruz, E. A. Pérez-García, J. A. Meave, β -Diversity and vegetation structure as influenced by slope aspect and altitude in a seasonally dry tropical landscape. *Landsc. Ecol.* **24**, 473–482 (2009).
26. M. Méndez-Toribio, G. Ibarra-Manríquez, A. Navarrete-Segueda, H. Paz, Topographic position, but not slope aspect, drives the dominance of functional strategies of tropical dry forest trees. *Environ. Res. Lett.* **12**, 085002 (2017).
27. G. P. Elliott, C. M. Cowell, Slope aspect mediates fine-scale tree establishment patterns at upper treeline during wet and dry periods of the 20th century. *Arct. Antarct. Alp. Res.* **47**, 681–692 (2015).
28. R. K. Danby, D. S. Hik, Variability, contingency and rapid change in recent subarctic alpine tree line dynamics. *J. Ecol.* **95**, 352–363 (2007).
29. A. Correa-Díaz, L. C. R. Silva, W. R. Horwath, A. Gómez-Guerrero, J. Vargas-Hernández, J. Villanueva-Díaz, A. Velázquez-Martínez, J. Suárez-Espinoza, Linking remote sensing and dendrochronology to quantify climate-induced shifts in high-elevation forests over space and time. *J. Geophys. Res. Biogeosci.* **124**, 166–183 (2019).
30. E. A. Ainsworth, S. P. Long, What have we learned from 15 years of free-air CO_2 enrichment (FACE)? A meta-analytic review of the responses of photosynthesis, canopy properties and plant production to rising CO_2 . *New Phytol.* **165**, 351–372 (2005).
31. J. C. Linares, J. J. Camarero, From pattern to process: Linking intrinsic water-use efficiency to drought-induced forest decline. *Glob. Chang. Biol.* **18**, 1000–1015 (2012).
32. D. McCarroll, N. J. Loader, Stable isotopes in tree rings. *Quat. Sci. Rev.* **23**, 771–801 (2004).
33. S. Szymczak, M. M. Joachimski, A. Bräuning, T. Hetzer, J. Kuhlemann, Are pooled tree ring $\delta^{13}\text{C}$ and $\delta^{18}\text{O}$ series reliable climate archives?—A case study of *Pinus nigra* spp. *laricio* (Corsica/France). *Chem. Geol.* **308–309**, 40–49 (2012).
34. P. B. Reich, M. B. Walters, B. D. Kloeppel, D. S. Ellsworth, Different photosynthesis–nitrogen relations in deciduous hardwood and evergreen coniferous tree species. *Oecologia* **104**, 24–30 (1995).
35. L. C. R. Silva, A. Gómez-Guerrero, T. Doane, W. Horwath, Isotopic and nutritional evidence for species- and site-specific responses to N deposition and elevated CO_2 in temperate forests. *J. Geophys. Res.* **120**, 1110–1123 (2015).
36. D. S. LeBauer, K. K. Treseder, Nitrogen limitation of net primary productivity in terrestrial ecosystems is globally distributed. *Ecology* **89**, 371–379 (2008).
37. C. Körner, Climatic treelines: Conventions, global patterns, causes (Klimatische Baumgrenzen: Konventionen, globale Muster, Ursachen). *Erdkunde* **61**, 316–324 (2007).
38. S. Hättenschwiler, I. T. Handa, L. Egli, R. Asshoff, W. Ammann, C. Körner, Atmospheric CO_2 enrichment of alpine treeline conifers. *New Phytol.* **156**, 363–375 (2002).
39. M. A. Dawes, F. Hagedorn, I. T. Handa, K. Streit, A. Ekblad, C. Rixen, C. Körner, S. Hättenschwiler, An alpine treeline in a carbon dioxide-rich world: Synthesis of a nine-year free-air carbon dioxide enrichment study. *Oecologia* **171**, 623–637 (2013).
40. L. U. Castruita-Esparza, L. C. R. Silva, A. Gómez-Guerrero, J. Villanueva-Díaz, A. Correa-Díaz, W. R. Horwath, Coping with extreme events: Growth and water-use efficiency of trees in western Mexico during the driest and wettest periods of the past one hundred sixty years. *J. Geophys. Res. Biogeosci.* **124**, 3419–3431 (2019).
41. T. M. Maxwell, L. C. R. Silva, A state factor model for ecosystem carbon–water relations. *Trends Plant Sci.* **25**, 652–660 (2020).
42. O. Sperling, L. C. R. Silva, A. Tixier, G. Théroux-Rancourt, M. A. Zwieniecki, Temperature gradients assist carbohydrate allocation within trees. *Sci. Rep.* **7**, 3265 (2017).
43. D. Salazar-tortosa, I. Querejeta, J. Castro, P. Villar-salvador, R. R. De Casas, L. Mat, A. Michelsen, The “isohydric trap”: A proposed feedback between water shortage, stomatal regulation, and nutrient acquisition drives differential growth and survival of European pines under climatic dryness. *Glob. Chang. Biol.* **24**, 4069–4083 (2018).
44. C. Sáenz-Romero, J.-B. Lamy, E. Loya-Rebollar, A. Plaza-Aguilar, R. Burlett, P. Lobit, S. Delzon, Genetic variation of drought-induced cavitation resistance among *Pinus hartwegii* populations from an altitudinal gradient. *Acta Physiol. Plant* **35**, 2905–2913 (2013).
45. L. D. S. L. O. R. Sternberg, Oxygen stable isotope ratios of tree-ring cellulose: The next phase of understanding. *New Phytol.* **181**, 553–562 (2009).
46. D. E. M. Ulrich, C. Still, J. R. Brooks, Y. Kim, F. C. Meinzer, Investigating old-growth ponderosa pine physiology using tree-rings, $\delta^{13}\text{C}$, $\delta^{18}\text{O}$, and a process-based model. *Ecology* **100**, e02656 (2019).
47. A. C. Finzi, E. H. DeLucia, J. G. Hamilton, D. D. Richter, W. H. Schlesinger, The nitrogen budget of a pine forest under free air CO_2 enrichment. *Oecologia* **132**, 567–578 (2002).
48. P. Millard, G. Grelet, Nitrogen storage and remobilization by trees: Ecophysiological relevance in a changing world. *Tree Physiology* **30**, 1083–1095 (2010).
49. G. P. Elliott, K. F. Kipfmüller, Multi-scale influences of slope aspect and spatial pattern on ecotonal dynamics at upper treeline in the Southern Rocky Mountains, U.S.A. *Arct. Antarct. Alp. Res.* **42**, 45–56 (2010).
50. K. C. Kelsey, S. H. Pedersen, A. J. Leffler, J. O. Sexton, M. Feng, J. M. Welker, Winter snow and spring temperature have differential effects on vegetation phenology and productivity across plant communities. *Glob. Chang. Biol.* **27**, 1572–1586 (2021).
51. J. M. Alexander, L. Chalmandrier, J. Lenoir, T. I. Burgess, F. Essl, S. Haider, C. Kueffer, K. McDougall, A. Milbau, M. A. Nuñez, A. Pauchard, W. Rabitsch, L. J. Rew, N. J. Sanders, L. Pellissier, Lags in the response of mountain plant communities to climate change. *Glob. Chang. Biol.* **24**, 563–579 (2018).

52. D. Palacios, L. García-Sancho, J. J. Zamorano, N. Andrés, A. Pintado, *EGU General Assembly Conference Abstracts* (2012), vol. 14, p. 3755.

53. L. C. R. Silva, H. Lambers, Soil-plant-atmosphere interactions: Structure, function, and predictive scaling for climate change mitigation. *Plant Soil*, 1–23 (2020).

54. H. J. B. Birks, W. Tinner, Past forests of Europe, in *European Atlas of Forest Tree Species*, J. SanMiguel-Ayanz, D. de Rigo, G. Caudullo, T. Houston Durrant, A. Mauri, Eds. (European Commission, 2016), pp. e010c45+.

55. B. C. McLaughlin, E. S. Zavaleta, Predicting species responses to climate change: Demography and climate microrefugia in California valley oak (*Quercus lobata*). *Glob. Chang. Biol.* **18**, 2301–2312 (2012).

56. S. Z. Dobrowski, A climatic basis for microrefugia: The influence of terrain on climate. *Glob. Chang. Biol.* **17**, 1022–1035 (2011).

57. E. Rehm, K. J. Feeley, Many species risk mountain top extinction long before they reach the top. *Front. Biogeogr.* **8**, e27788 (2016).

58. R. Bobbink, G. W. Heil, G. W. Heil, R. Bobbink, N. Trigo Boix, in *Ecology and Man in Mexico's Central Volcanoes Area* (Springer, 2003), pp. 1–18.

59. A. G. Bunn, A dendrochronology program library in R (dplR). *Dendrochronologia* **26**, 115–124 (2008).

60. R. L. Peters, P. Groenendijk, M. Vlam, P. A. Zuidema, Detecting long-term growth trends using tree rings: A critical evaluation of methods. *Glob. Chang. Biol.* **21**, 2040–2054 (2015).

61. A. Gessler, J. P. Ferrio, R. Hommel, K. Treydte, R. A. Werner, R. K. Monson, Stable isotopes in tree rings: towards a mechanistic understanding of isotope fractionation and mixing processes from the leaves to the wood. *Tree Physiol.* **34**, 796–818 (2014).

62. G. D. Farquhar, M. H. O'leary, J. A. Berry, On the relationship between carbon isotope discrimination and the intercellular carbon dioxide concentration in leaves. *Funct. Plant Biol.* **9**, 121–137 (1982).

63. L. C. R. Silva, W. R. Horwath, Explaining global increases in water use efficiency: Why have we overestimated responses to rising atmospheric CO₂ in natural forest ecosystems? *PLOS ONE* **8**, e53089 (2013).

64. D. McCarroll, M. H. Gagen, N. J. Loader, I. Robertson, K. J. Anchukaitis, S. Los, G. H. F. Young, R. Jalkanen, A. Kirchhefer, J. S. Waterhouse, Correction of tree ring stable carbon isotope chronologies for changes in the carbon dioxide content of the atmosphere. *Geochim. Cosmochim. Acta* **73**, 1539–1547 (2009).

65. W. Peters, A. R. Jacobson, C. Sweeney, A. E. Andrews, T. J. Conway, K. Masarie, J. B. Miller, L. M. P. Bruhwiler, G. Pétron, A. I. Hirsch, D. E. J. Worthy, G. R. van der Werf, J. T. Randerson, P. O. Wennberg, M. C. Krol, P. P. Tans, An atmospheric perspective on North American carbon dioxide exchange: CarbonTracker. *Proc. Natl. Acad. Sci. U.S.A.* **104**, 18925–18930 (2007).

66. F. Biondi, F. Qeadan, A theory-driven approach to tree-ring standardization: Defining the biological trend from expected basal area increment. *Tree Ring Res.* **64**, 81–96 (2008).

67. D. Bates, M. Maechler, B. Bolker, lme4: Linear mixed-effects models using S4 classes, 2011. *R Packag. version 0.999375-42* (2012); <http://CRAN.R-project.org/package=lme4>.

68. S. N. Wood, *Generalized Additive Models: An Introduction with R* (CRC Press, 2017).

Acknowledgments: We thank A. Gómez-Guerrero from El Colegio de Postgrados in Mexico, J. Villanueva from CENID-RASPA INIFAP, and L. Vazquez-Selem from the Institute of Geography at the National Autonomous University of Mexico (UNAM) for guidance in the design of the study and technical and analytical support. We also thank L. de Wit, T. Maxwell, M. Deluna, A. Draime, L. Hansen, R. Keeny, T. Marlatt, D. Nguyen, K. Sheehy, C. Shepherd, and B. Thurman. **Funding:** We thank UC MEXUS for providing financial support for this project.

Author contributions: P.Q. wrote the paper, conducted fieldwork and laboratory work, analyzed the data, and designed the study. L.C.R.S. wrote the paper, conducted laboratory work, and analyzed and interpreted the data. E.S.Z. designed the study, interpreted the data, and edited the paper. **Competing interests:** The authors declare that they have no competing interests. **Data and materials availability:** All data needed to evaluate the conclusions in the paper are present in the paper and/or the Supplementary Materials. Original data can also be found at Quadri, Paulo (2020), Climate-induced reversal of tree growth patterns in a high-elevation tropical forest (GitHub: <https://github.com/Liquidambar99/Climate-induced-reversal-of-tree-growth-patterns-in-a-high-elevation-tropical-forest>).

Submitted 17 March 2020

Accepted 8 April 2021

Published 26 May 2021

10.1126/sciadv.abb7572

Citation: P. Quadri, L. C. R. Silva, E. S. Zavaleta, Climate-induced reversal of tree growth patterns at a tropical treeline. *Sci. Adv.* **7**, eabb7572 (2021).

Climate-induced reversal of tree growth patterns at a tropical treeline

Paulo QuadriLucas C. R. SilvaErika S. Zavaleta

Sci. Adv., 7 (22), eabb7572. • DOI: 10.1126/sciadv.abb7572

View the article online

<https://www.science.org/doi/10.1126/sciadv.abb7572>

Permissions

<https://www.science.org/help/reprints-and-permissions>